

# Structural Changes in Early Photolysis Intermediates of Rhodopsin from Time-Resolved Spectral Measurements of Artificial Pigments Sterically Hindered along the Chromophore Chain

James W. Lewis,<sup>†</sup> Iddo Pinkas,<sup>‡</sup> Mordechai Sheves,<sup>\*,‡</sup> Michael Ottolenghi,<sup>§</sup> and David S. Kliger<sup>\*,†</sup>

Contribution from the Department of Chemistry and Biochemistry, University of California, Santa Cruz, California 95064, Department of Organic Chemistry, Weizmann Institute of Science, Rehovot 76 100, Israel, and Department of Physical Chemistry, The Hebrew University of Jerusalem, Jerusalem 91 904, Israel

Received July 18, 1994<sup>Ⓞ</sup>

**Abstract:** Kinetic spectra of early photolysis intermediates were monitored after nanosecond laser photolysis of a series of artificial visual pigments containing retinal analogs with bulky substituents along the polyene chain. Time-resolved absorbance changes over the spectral range 400–700 nm were recorded at discrete times from 20 ns to 5  $\mu$ s following room temperature excitation with a pulse of 477 nm light. Photolysis of bovine rhodopsin regenerated with 9-ethyl-9-*cis*-retinal, 19,11-ethano-11-*cis*-retinal, or 13-ethyl-9-*cis*-retinal produced intermediates similar to those seen after rhodopsin photolysis, i.e. bathorhodopsin (Batho)  $\rightleftharpoons$  blue-shifted intermediate (BSI)  $\rightarrow$  lumirhodopsin (Lumi). In contrast to previously studied artificial pigments and rhodopsin itself, for these chromophores with bulky substituents, the equilibrium between Batho and BSI is back-shifted. The stability of BSI relative to Batho is most affected in the 13-ethyl pigment, which had an equilibrium constant of 0.4, approximately one-third of the value observed for rhodopsin. As the bulky substituent moves toward the C9 end of the chromophore,  $K_{eq}$  moves toward the rhodopsin value, with the result for the locked 9-*trans*-rhodopsin pigment being intermediate between those of the 9-ethyl and 13-ethyl pigments. The presence of bulky substituents also slows the microscopic rate of Batho decay. This effect is largest for the 9-ethyl pigment whose Batho decay is slowed by a factor of 5. Freedom of movement of the 9-methyl (restricted in the 9-ethyl case) is proposed to control the rate of Batho decay in a mechanism involving passage of the chromophore's C8-hydrogen by the 5-methyl group of its  $\beta$ -ionone ring to form BSI. For all these pigments, the decay of BSI is substantially slower than for previous pigments, indicating that steric hindrance along the polyene chain interferes with the protein change triggered by BSI formation and suggesting that the protein change may involve side chains adjacent to this region of the chromophore.

Wald and co-workers originally showed that light-induced 11-*cis* to *all-trans* isomerization of the retinal chromophore triggers visual transduction in rhodopsin.<sup>1</sup> Since this event does not significantly alter the chemical properties of the chromophore, protein structural changes subsequent to isomerization must be driven by the shape change of the chromophore within its binding pocket. Systematic studies to determine which synthetic retinal analogs form artificial pigments have led to a crude picture of the shape of rhodopsin's chromophore binding pocket.<sup>2</sup> The results of that work show some regions of the pocket to be crowded, preventing synthetic pigment formation with chromophores extending into those regions. In contrast, other areas of the pocket seem to have sufficient flexibility to accommodate structures that differ substantially from 11-*cis*-retinal. In particular, studies have shown space to exist below

the polyene chain, as drawn in Figure 1, at the 5-methyl<sup>3</sup> and 13-methyl<sup>4</sup> positions and also above the chain at the 9-methyl position.<sup>2a,5</sup> The amount of free space that has been found and its distribution at specific places within the pocket raise the question of how these various spaces affect the events subsequent to isomerization. Such a question can best be answered by kinetic studies under physiologically relevant conditions. The approach taken here is to prepare synthetic visual pigments with chromophores that fill up some of the vacant space in the pocket with alkyl substituents along the polyene chain. Comparison of the decay rates of the early photolysis intermediates of these sterically hindered pigments with the analogous decay rates in native rhodopsin reveals the processes that make use of the "free" volume in the pocket.

Kinetic studies of absorbance changes following rhodopsin photolysis have led to a model in which bathorhodopsin (Batho) decays into an equilibrium with a blue-shifted intermediate (BSI), which then decays irreversibly to lumirhodopsin (Lumi).<sup>6</sup>

<sup>†</sup> University of California at Santa Cruz.

<sup>‡</sup> Weizmann Institute of Science.

<sup>§</sup> The Hebrew University of Jerusalem.

<sup>Ⓞ</sup> Abstract published in *Advance ACS Abstracts*, January 1, 1995.

(1) (a) Orshnik, W.; Brown, P. K.; Hubbard, R.; Wald, G. *Proc. Natl. Acad. Sci. U.S.A.* **1956**, *42*, 578–580. (b) Yoshizawa, T.; Wald, G. *Nature (London)* **1963**, *197*, 1279–1286.

(2) (a) Liu, R. S. H.; Asato, A. The Binding Site of Opsin Based on Analog Studies with Isomeric, Fluorinated, Alkylated, and Other Modified Retinals. In *Chemistry and Biology of Synthetic Retinoids*; Dawson, M. I., Okamura, W. H., Eds.; CRC Press: Boca Raton, FL, 1989; Chapter 3, pp 52–75. (b) Derguini, F.; Nakanishi, K. *Photobiochem. Photobiophys.* **1986**, *13*, 259–283. (c) Ottolenghi, M.; Sheves, M. *J. Membr. Biol.* **1989**, *112*, 193–212.

(3) Asato, A. E.; Zhang, B.-W.; Denny, M.; Mirzadegan, T.; Seff, K.; Liu, R. S. H. *Bioinorg. Chem.* **1989**, *17*, 410–421.

(4) Nakanishi, K. *Pure Appl. Chem.* **1985**, *57*, 769–776.

(5) Balogh-Nair, V.; Nakanishi, K. Visual Pigment and Bacteriorhodopsin Analogs. In *Chemistry and Biology of Synthetic Retinoids*; Dawson, M. I., Okamura, W. H., Eds.; CRC Press: Boca Raton, FL, 1989; Chapter 7, pp 147–176.

(6) Hug, S. J.; Lewis, J. W.; Einterz, C. M.; Thorgeirsson, T. E.; Kliger, D. S. *J. Am. Chem. Soc.* **1990**, *112*, 1475–1485.

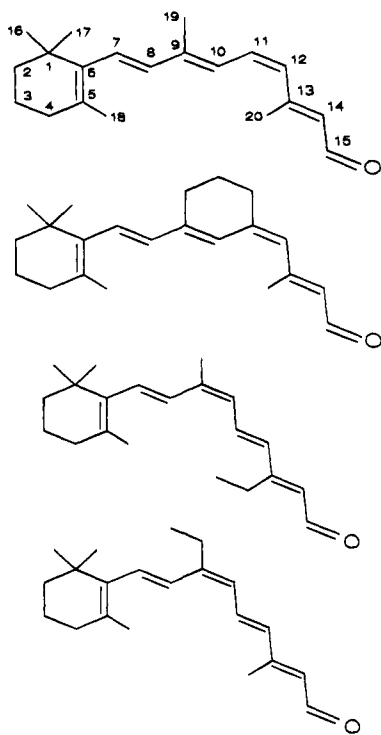


**Figure 1.** Chromophore structures. From top to bottom: 11-*cis*-retinal, the chromophore of rhodopsin; 19,11-ethano-11-*cis*-retinal, the chromophore of locked 9-*trans*-rhodopsin; 13-ethyl-9-*cis*-retinal, the chromophore of 13-ethylisorhodopsin; and 9-ethyl-9-*cis*-retinal, the chromophore of 9-ethylisorhodopsin.

A considerable amount has been learned about the structure of Batho from resonance Raman spectroscopy.<sup>7</sup> Those measurements show that Batho trapped at low temperatures displays hydrogen-out-of-plane bending (HOOP) modes characteristic of an *all-trans* chromophore that has been torsionally strained. Less is known about the structure of BSI, but evidence suggests that formation of BSI triggers protein change, making it a key intermediate in our understanding of receptor function.<sup>8</sup>

Previous studies with artificial visual pigments have indicated the presence of BSI and have shown that modified chromophores such as 13-demethylretinal or 5,6-dihydroretinal accelerate Batho decay and favor BSI in the Batho–BSI equilibrium.<sup>8</sup> The availability of artificial pigments that form stable BSI's at low temperature is of practical importance since it has allowed BSI characterization with FTIR. The FTIR spectra show reduced HOOP modes, indicating that chromophore torsion has relaxed at BSI.<sup>9</sup> The common feature of chromophores studied to date, which favor BSI, is that they fit the pocket more loosely through either increased flexibility or decreased bulk. In the study reported here, we take the opposite approach and study chromophores that fit the pocket more tightly than previous retinal analogs or retinal itself. The three synthetic chromophores used here are shown in Figure 1. One of these, 19,11-ethano-11-*cis*-retinal, was studied previously<sup>10</sup> since it could be used to establish whether a 10-*s-cis* intermedi-

ate was obligatory in the bleaching pathway. For those studies, sufficient pigment was made to confirm that locked 9-*trans*-rhodopsin made from 19,11-ethano-11-*cis*-retinal did indeed bleach, forming a Batho intermediate.<sup>10</sup> At that time, the amount of pigment available was insufficient for complete characterization of all intermediates using the available apparatus. Since then, a much more efficient photolysis system has been developed,<sup>11</sup> and here this is used to extend the previous measurements to characterization of the BSI formed from the 19,11-ethano-11-*cis*-retinal chromophore. The results of these more detailed studies, combined with those from pigments formed from 9-ethyl-9-*cis*-retinal and 13-ethyl-9-*cis*-retinal, show that alkyl bulk slows the early and/or late phases of Batho decay with the effect depending on whether the substituent is at the C9 or C13 end of the polyene chain, respectively.

## Experimental Section

19,11-Ethano-11-*cis*-retinal was prepared as previously described.<sup>12</sup> 9-Ethyl-9-*cis*-retinal was synthesized by methylating  $\beta$ -ionone at its methyl ketone position using sodium amide and methyl iodide. The product was reacted with the sodium salt of (diethylphosphono)acetonitrile, followed by reduction of the nitrile group to an aldehyde by diisobutylaluminum hydride. The *cis* isomer was separated by flash chromatography, converted to 9-ethyl-9-*cis*-retinal using the sodium salt of 3-methyl-4-phosphonocrotonitrile, and reduced with diisobutylaluminum hydride.

13-Ethyl-9-*cis*-retinal was prepared by condensing 5-(2,6,6-trimethyl-1-cyclohexen-1-yl)-3-methyl-2-*cis*-penta-2,4-dien-1-al with ethyl methyl ketone in the presence of potassium hydroxide. The resulting ketone was converted to a 13-ethyl-9-*cis*-retinal by condensation with the sodium salt of (diethylphosphono)acetonitrile and reduction with diisobutylaluminum hydride.

Opsin for regeneration was prepared by bleaching suspensions of bovine rod outer segments (ROS) in buffer (pH 7.0 10 mM TRIS, 60 mM KCl, 30 mM NaCl, 2 mM MgCl<sub>2</sub>, 0.1 mM EDTA) containing 50 mM hydroxylamine for 2 min with a 25 W light bulb. After it was bleached, the ROS received three cycles of pelleting (Sorvall SS-34 rotor, 30 min at 17 K rpm) followed by resuspension in buffer to remove unreacted hydroxylamine. Subsequent steps were conducted in darkness or under dim red light. Chromophore was added in 2-3-fold excess (by optical density) over the amount of opsin present. Samples were incubated at 37 °C for 1 h, after which, residual excess chromophore was converted to the alcohol form by adding approximately 0.1 mg of NADPH/mg of opsin and continuing the incubation for an additional hour. Yields of the pigments varied somewhat from batch to batch with typical values being 50% for 13-ethyl-9-*cis*-retinal, 25% for 9-ethyl-9-*cis*-retinal, and 15% for 19,11-ethano-11-*cis*-retinal. The  $\lambda_{\max}$  values of the pigments obtained are given in Table 3. In reading the table, note that the 11-*cis* chromophore produces a rhodopsin analog while the 9-*cis* chromophores produce isorhodopsin analogs. Blank regenerations showed a complete absence of any regeneration without added chromophore. Regenerated ROS were stripped of extrinsic membrane proteins by two cycles of pelleting followed by resuspension in 1 mM EDTA solution, which had been adjusted to pH 7.0. For photolysis measurements, the ROS were pelleted and then resuspended in a sufficient volume of 2% octyl glucoside in buffer to produce a sample whose absorbance was  $\sim 0.6$  in 1 cm path length at the peak of the long wavelength pigment absorption band.

Difference absorption spectra were collected at varying time delays after sample photolysis with a 7 ns pulse of 477 nm light from a dye laser pumped by the third harmonic of a Nd:YAG laser (fluence 50  $\mu\text{J}/\text{mm}^2$ ). Samples were replaced after each photolysis pulse, but for the locked 9-*trans* pigment, too little pigment was available for

(7) Palings, I.; Pardo, J. A.; van den Berg, E.; Winkel, C.; Lugtenberg, J.; Mathies, R. A. *Biochemistry* **1986**, *26*, 2544–2556.

(8) Randall, C. E.; Lewis, J. W.; Hug, S. J.; Björling, S.; Elsner-Shanas, I.; Friedman, N.; Ottolenghi, M.; Sheves, M.; Kliger, D. S. *J. Am. Chem. Soc.* **1991**, *113*, 3473–3485.

(9) (a) Ganter, U. M.; Gärtner, W.; Siebert, F. *Eur. Biophys. J.* **1990**, *18*, 295–299. (b) Ganter, U. M.; Kashima, T.; Sheves, M.; Siebert, F. *J. Am. Chem. Soc.* **1991**, *113*, 4087–4092.

(10) Sheves, M.; Albeck, A.; Ottolenghi, M.; Bovee-Geurts, P. H. M.; De Grip, W. J.; Elnterz, C. M.; Lewis, J. W.; Schaechter, L. E.; Kliger, D. S. *J. Am. Chem. Soc.* **1986**, *108*, 6440–6441.

(11) Lewis, J. W.; Kliger, D. S. *Rev. Sci. Instrum.* **1993**, *64*, 2828–2835.

(12) Albeck, A.; Friedman, N.; Sheves, M.; Ottolenghi, M. *J. Am. Chem. Soc.* **1986**, *108*, 4614.

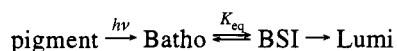
characterization with the 24  $\mu\text{L}$  per pulse system<sup>13</sup> used in previous work as well as for the 9-ethyl and 13-ethyl pigments here. Thus, a recently developed<sup>11</sup> 1  $\mu\text{L}$  microscale system was used for this pigment. With the micro system, more scattered laser light was encountered so that the earliest time at which difference spectra could be collected was 30 ns instead of 20 ns for the larger sample system. Another important difference between these systems was the 0.2 cm optical path length for the micro system vs the 1.0 cm optical path length in the previous apparatus. In all cases, absorbance changes due to rotational diffusion were eliminated either by averaging parallel and perpendicular absorbances (9-ethyl and 13-ethyl pigments) or by measuring with light linearly polarized at the magic angle ( $54.7^\circ$ ) relative to the polarization of the actinic light (locked 9-*trans*). All measurements were conducted at room temperature.

Difference spectra were fit globally to sums of exponential functions with one, two, or three lifetimes using a previously described method.<sup>6</sup> In most cases, fits to three exponentials did not converge, and in no case was a stable three-exponential fit found for these pigments. The number of exponentials giving the best fit to the data was determined from plots of residuals. Once the number of exponentials was determined, absolute spectra of the intermediates could be determined from the time-dependent spectra associated with the individual rates and the spectrum of the material bleached by the laser.<sup>6,14</sup> For the purpose of determining the  $\lambda_{\text{max}}$  values of the intermediates, the resulting spectra were fit to a Gaussian function using a Simplex fitting routine (The Math Works, Sherborn, MA 01770). Molecular modeling of the retinal chromophore was performed using Hyperchem software (Aurora, Sausalito, CA 94965).

## Results

The data collected here consist of absorbance difference spectra (sample absorbance at time  $t$  after photolysis minus sample absorbance prior to photolysis). All wavelengths from 400 to 700 nm are monitored simultaneously with the 10 ns gate of the OMA image intensifier acting to provide time resolution. A high signal-to-noise ratio in the spectra is achieved by using an extremely bright, ultrastable flash lamp to produce white light for the probe source. The 0.2% reproducibility of the flashes allows measurements to be made in single beam mode with a minimum amount of signal averaging.

Difference spectra collected at varying times after photolysis of 9-ethylisrorhodopsin are shown in Figure 2a. Compared with rhodopsin (see Table 1), substantially slower kinetics are observed for this pigment, as shown by the lack of change between the 20 and 40 ns difference spectra. Optical changes in this pigment also continue to later times compared with optical changes in rhodopsin, for which much smaller changes occur between 640 ns and 1.28  $\mu\text{s}$ .<sup>6</sup> The shifting isosbestic point, from  $\sim 485$  nm at early times to  $\sim 510$  nm later, is evidence for at least two processes occurring, and the data are best fit using a biexponential model with decay lifetimes of 120 and 770 ns (compared with lifetimes for rhodopsin of 30 and 220 ns). Aside from the slower kinetics, the qualitative features of the spectra are the same as those obtained for rhodopsin, i.e. an initial Batho product that decays with a red-shifting isosbestic point to a blue-shifted product. These similarities justify analysis of the data in terms of the scheme that has been established for rhodopsin.



Application of this scheme to the data to obtain absolute spectra of the intermediates requires that an estimate of the equilibrium constant be made. Constraints on this estimate are provided

(13) Einterz, C. M.; Lewis, J. W.; Kliger, D. S. *Proc. Natl. Acad. Sci. U.S.A.* **1987**, *84*, 3699–3703.

(14) Albeck, A.; Friedman, N.; Ottolenghi, M.; Sheves, M.; Einterz, C. M.; Hug, S. J.; Lewis, J. W.; Kliger, D. S. *Biophys. J.* **1989**, *55*, 233–241.

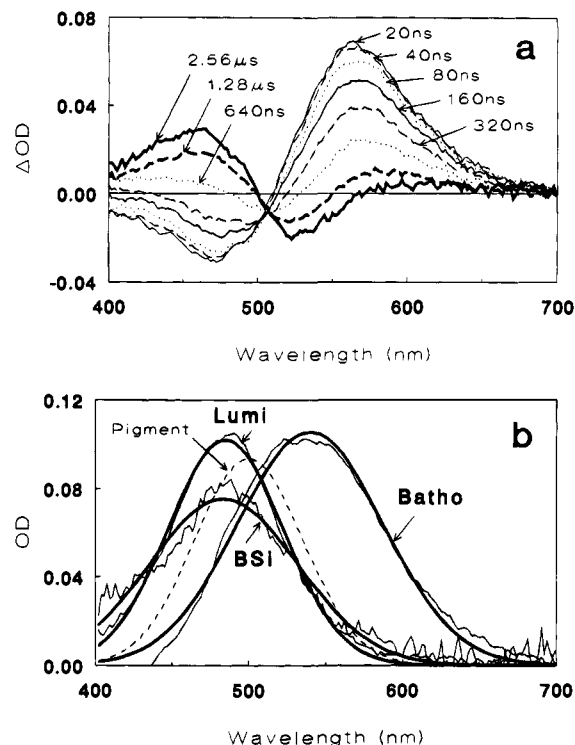


**Figure 2.** (a) Absorbance difference spectra observed after photolysis of 9-ethylisrorhodopsin. Difference spectra were collected at the specified time delay after photolysis of samples with a pulse of 477 nm light. These data were collected in a 1 cm path length cuvette. (b) Absorbance spectra of the intermediate species produced after photolysis of 9-ethylisrorhodopsin. The intermediate's spectra were calculated from the difference spectra shown in part (a) using the observed lifetimes given in Table 1 and a Batho  $\rightleftharpoons$  BSI equilibrium constant of 0.9. The dashed line shows the spectrum of the pigment that was photolyzed to produce these intermediates. The Gaussian functions' fits to the intermediate spectra are shown by the heavy lines in this figure. The parameters describing these Gaussian functions are given in Table 3.

**Table 1.** Observed Lifetimes

plgnt	Batho $\rightleftharpoons$ BSI (ns)	[Batho $\rightleftharpoons$ BSI] $\rightarrow$ Lumi
rhodopsin <sup>6</sup>	30 $\pm$ 7	220 $\pm$ 20 ns
isorhodopsin <sup>a</sup>	37 $\pm$ 7	186 $\pm$ 20 ns
9-ethylisrorhodopsin	120 $\pm$ 30	770 $\pm$ 100 ns
locked 9- <i>trans</i> -rhodopsin	43 $\pm$ 10	1.2 $\pm$ 0.2 $\mu\text{s}$
13-ethylisrorhodopsin	30 $\pm$ 10	1.7 $\pm$ 0.2 $\mu\text{s}$

<sup>a</sup> Hug, S. J. Ph.D. Dissertation, University of California, Santa Cruz, CA, 1989.

by the requirement that the absolute spectra obtained be real, nonnegative, and have roughly Gaussian band shape. When these criteria are applied, the value of  $K_{\text{eq}}$  appropriate for rhodopsin, 1.4, is found to be too large for 9-ethylisrorhodopsin. Instead, the most reasonable intermediate spectra are obtained for  $K_{\text{eq}} \sim 0.9$ . The absolute intermediate spectra that result from use of this value are shown in Figure 2b. The microscopic rates associated with these intermediates are tabulated in Table 2. Note that, as is usual for this type of kinetic scheme, the reciprocal of the microscopic rate of BSI decay gives a BSI lifetime significantly smaller than the slow observed lifetime. This occurs because the BSI pool that decays to Lumi in our experiment is continually replenished from the Batho pool that is in equilibrium with it. This influx slows the observed rate of BSI decay from the microscopic value.

Difference spectra obtained from locked 9-*trans*-rhodopsin are shown in Figure 3a. Here, too, the initial photoproduct is red-shifted, but its decay is faster than in the 9-ethylisrorhodopsin

**Table 2.** Equilibrium Constants and Reciprocal Microscopic Rates

pigment	$K_{eq}$	Batho $\rightarrow$ BSI (ns)	Batho $\leftarrow$ BSI (ns)	BSI $\rightarrow$ Lumi (ns)
rhodopsin <sup>6</sup>	1.4	74	107	105
isorhodopsin <sup>a</sup>	2.0	67	134	103
9-ethylisorhodopsin	0.9	400	360	230
locked 9- <i>trans</i> -rhodopsin	0.5	140	70	360
13-ethylisorhodopsin	0.4	100	40	460

<sup>a</sup> Hug, S. J. Ph.D. Dissertation, University of California, Santa Cruz, CA, 1989.

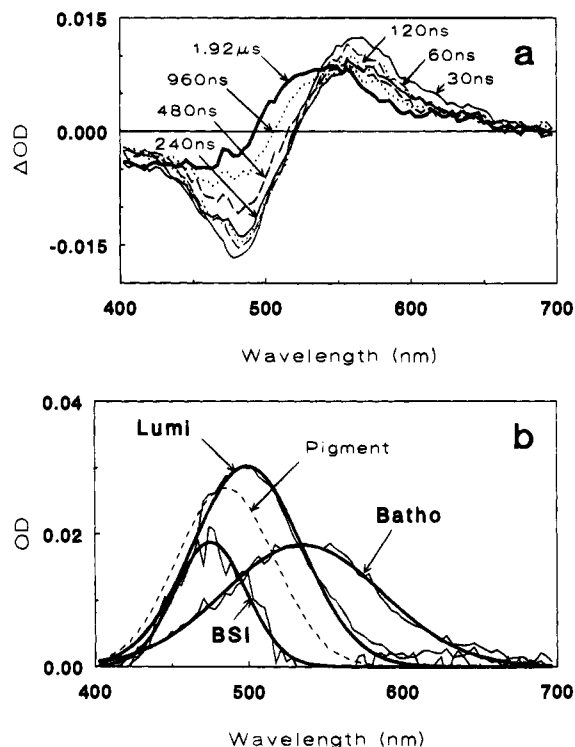


**Figure 3.** (a) Absorbance difference spectra observed after photolysis of locked 9-*trans*-rhodopsin. Difference spectra were collected at the specified time delay after photolysis of samples with a pulse of 477 nm light. These data were collected in a 0.2 cm path length cuvette (the microscale apparatus). (b) Absorbance spectra of the intermediate species produced after photolysis of locked 9-*trans*-rhodopsin. The Batho  $\rightleftharpoons$  BSI equilibrium constant of 0.5 was used to produce these spectra. Line types and other details are similar to Figure 2b.

**Table 3.**  $\lambda_{max}$  Values (nm)

pigment	pigment	Batho	BSI	Lumi
rhodopsin <sup>6</sup>	498	529	477	492
isorhodopsin <sup>a</sup>	483	530	475	485
9-ethylisorhodopsin	500	540	483	485
locked 9- <i>trans</i> -rhodopsin	482	535	475	499
13-ethylisorhodopsin	488	539	498	489

<sup>a</sup> Hug, S. J. Ph.D. Dissertation, University of California, Santa Cruz, CA, 1989.

case, so that the transient absorbance increase detected in the earliest difference spectrum is smaller by comparison. The lifetimes obtained from a two-exponential fit were 43 ns and 1.2  $\mu$ s. For locked 9-*trans*-rhodopsin, an even smaller  $K_{eq}$  value,  $\sim$ 0.5, was required to produce reasonable intermediate spectra. The results are shown in Figure 3b and Table 3.

Difference spectra obtained from 13-ethylisorhodopsin are shown in Figure 4a. Again, a shifting isosbestic point gives evidence that at least two processes occur, but for this pigment, the direction of the shift is opposite to the direction seen in the other two pigments or in rhodopsin itself. When these data are fit to two exponentials, lifetimes of 30 ns and 1.7  $\mu$ s result.

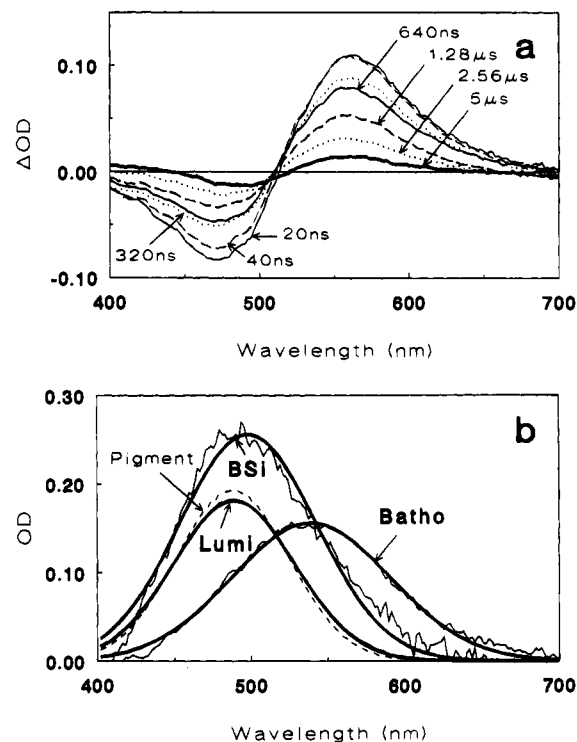


**Figure 4.** (a) Absorbance difference spectra observed after photolysis of 13-ethylisorhodopsin. Difference spectra were collected at the specified time delay after photolysis of samples with a pulse of 477 nm light. These data were collected in a 1 cm path length cuvette. (b) Absorbance spectra of the intermediate species produced after photolysis of 13-ethylisorhodopsin. The Batho  $\rightleftharpoons$  BSI equilibrium constant of 0.4 was used to produce these spectra. Line types and other details are similar to Figure 2b.

The best intermediate spectra result from a  $K_{eq}$  choice of  $\sim$ 0.4, and the spectral and kinetic results are given in Figure 4b and Table 3. The spectrum of 13-ethylisorhodopsin BSI is unusual both in its lack of blue shift and in its relatively large absorption intensity compared with the other intermediates. This change from the usual characteristics of BSI directly causes the reversed direction of the isosbestic shift observed in the raw data. For all pigments, wavelengths of maximum absorbance of all intermediates are given in Table 3.

## Discussion

The group of synthetic pigments studied here have the common characteristic that bulky alkyl substituents have been added along the polyene chain. Since the Batho intermediate contains a twisted polyene chromophore<sup>7</sup> and Batho decay relaxes this twist, resulting in less well-characterized successor structures, it was of interest to determine how bulky substituents affect Batho decay. Previous synthetic pigment studies, principally with chromophores modified to introduce flexibility (dihydro) or reduce bulk along the polyene chain (demethyl), found accelerated Batho decay accompanied by forward shift of the Batho  $\rightleftharpoons$  BSI equilibrium.<sup>8</sup> The microscopic BSI decay



rate, in contrast, was relatively unaffected by those chromophore modifications, leading to the idea that this rate was limited not by the chromophore but by protein change. On the basis of previous synthetic pigment results, it is not surprising, therefore, that the introduction of bulky substituents should slow decay of Batho and back shift the Batho  $\rightleftharpoons$  BSI equilibrium. The accompanying slowing of the BSI decay was less predictable, but in retrospect, it is reasonable that bulky side chains would interfere with release of constraints to protein motion when BSI is formed. The general picture that emerges from the data presented here is that bulky substituents, at least at odd carbons C9–C13, slow the forward reactions of both Batho and BSI.

Beyond this general picture, the data reveal a more specific relationship between substituent position and the processes that are principally affected. The C9 position has the largest effect on the earliest reaction, Batho decay. Examination of the microscopic rates in Table 2 shows that bulk at the C9 position primarily slows interconversion of Batho and BSI. With respect to the subsequent decay of BSI to Lumi, however, steric effects at the C9 position are relatively less important. As the position of the bulky substituent moves toward the C13 position in the sequence of chromophores studied here, the specificity for Batho and BSI forward rates is reversed so the BSI decay rate is more perturbed than its formation rate. Even more pronounced as the substituent moves from C9 to C13 is the effect on the Batho  $\leftarrow$  BSI rate. It goes from substantially slower for 9-ethylisorhodopsin to significantly faster than the rhodopsin rate for 13-ethylisorhodopsin. To a first approximation then, bulk at the C9 position primarily raises the activation energy for the Batho–BSI reaction, while bulk at the C13 position affects later stages, raising the free energy of BSI relative to Batho (as shown by the back shifting of  $K_{eq}$ ) and raising the activation energy for BSI decay to Lumi. The specific picture is one of sequential change, first at the C9 position then at the C13 position.

Since the alkyl substituents used here are likely to act by selectively restricting access to space within the protein pocket containing the chromophore, the observed substituent effects can be understood in terms of the shape of the pocket and should give information about structural characteristics of the chromophore in each of the intermediates. Consideration of the various chromophore analogs that form visual pigments has led to a fairly detailed picture of the pocket occupied by 9-*cis* and 11-*cis* isomers.<sup>2a</sup> Of course, at Batho the chromophore shape has changed significantly, creating strained contacts, but FTIR studies<sup>9a</sup> suggest that the pocket shape does not change until after Batho has decayed. Otherwise, it is difficult to understand what constrains the highly strained form of the chromophore that is known to be characteristic of Batho.<sup>7</sup> Chromophore analog binding studies have pointed to the existence of “weak” spots at various points in the pocket wall where bulk added to synthetic chromophores does not seriously interfere with pigment formation. One such area is above the 9-methyl group of the 11-*cis* chromophore. Naively, such a weak spot might be thought to accommodate chromophore displacement at Batho, but such accommodation is hard to reconcile with the requirement that energy be stored by Batho. In fact, comparison of chromophore models of rhodopsin and Batho presented in Figure 5 shows that it is likely that the 9-methyl pulls away from the pocket wall at Batho, creating even more free space above the 9-methyl than exists in rhodopsin. The kinetic results for 9-ethylisorhodopsin indicate that creation of this free volume is important for Batho decay since filling the space by increasing the bulk of the side chain at the C9 position dramatically slows Batho–BSI interconversion. The question then becomes what

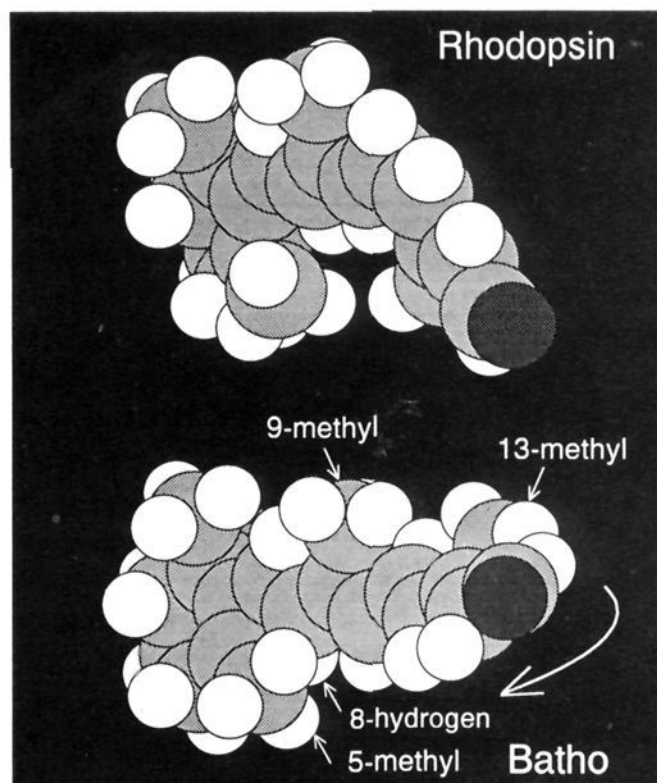


**Figure 5.** Model of retinal chromophore in rhodopsin and bathorhodopsin. In rhodopsin (top), the 11-*cis*-retinylidene chromophore twists slightly around the 6–7 single bond to relieve the contact between the C8-hydrogen and the 5-methyl group of the  $\beta$ -ionone ring. After isomerization (bottom), the *all-trans*-retinylidene chromophore is twisted with the torsion shown by the curved arrow. The twist forces the C8-hydrogen into the 5-methyl of the ring, and this barrier is proposed to constitute the barrier between Batho and BSI. From the view given in this figure, the importance of the 9-methyl for this barrier can be seen. The data presented here show that substitution with an ethyl group at the C9 position slows the formation of BSI. This substitution interferes with the upward motion of C9 required to pass the C8-hydrogen over the ring 5-methyl.

chromophore-localized energetic barrier would be affected by the free volume above the 9-methyl?

The viewing angle of the bathorhodopsin chromophore in Figure 5 has been chosen to give insight into this question. As viewed, torsion has been introduced into the polyene chain at the Batho stage by a 60° clockwise twist of the portion of the chromophore on the protein side of C10. This twist is then distributed in 20° increments over the three single bonds, C14–C15, C12–C13, and C10–C11.<sup>7</sup> The net effect of these twists can be seen as pushing the 8-hydrogen into the 5-methyl of the  $\beta$ -ionone ring. This contact is a likely candidate for the barrier to BSI formation. Support for the conclusion that the barrier is in this region of the chromophore comes from previous results indicating that the Batho–BSI barrier is reduced by introduction of flexibility into the ring (5,6-dihydroisorhodopsin) and, more specifically, when the double bond is moved away from the C5–C6 position even with constant ring flexibility ( $\alpha$ -isorhodopsin). In the present context, it is also clear that the 8-hydrogen–5-methyl contact would be very dependent on the volume available in the pocket above the 9-methyl since the 8-hydrogen is rigidly linked to the 9-methyl. Presumably, movement of the 8-hydrogen past the 5-methyl would relieve the polyene twist that gives rise to the HOOP modes of Batho, and indeed, reduced HOOP modes have been reported in the FTIR spectra of synthetic pigments that form stable BSI intermediates at low temperature.<sup>9</sup> Relaxation of twist during BSI formation is also consistent with the reduction of normal mode frequencies, which is potentially responsible for the entropic stabilization of this intermediate relative to Batho.

While the kinetic barrier between Batho and BSI is controlled by 9-methyl motion, the equilibrium energetics of these two intermediates seem to be more affected by the steric situation

at the 13-methyl position. Apparently, at BSI the C13 substituent has moved to a region of the pocket that is more confined than the region occupied by the C13 substituent in Batho. Synthetic chromophore binding studies with the 12-methyl analog of retinal have shown that the vicinity of the C12 position in the 11-*cis* pigment is so crowded that negligible amounts of pigment form even though the 9-*cis* isomer readily forms a pigment.<sup>15</sup> This has been interpreted as an indication of rigidity of the pocket near the chromophore's 12-hydrogen. Comparison of the chromophore structures shown in Figure 5 shows that the motion of the polyene chain as the 8-hydrogen-5-methyl contact pushes through to form BSI would potentially carry the 13-ethyl into the same unfavorable region of the pocket originally occupied by the 12-hydrogen. Therefore, the crowding that prevents pigment formation from 11-*cis*-12-methylretinal may be the same interaction that makes the Batho-BSI equilibrium so unfavorable in the 13-ethylisorhodopsin case. This analysis of chromophore motion seems attractive based on the kinetic parameters measured here, but ultimately, the validity of such a model must rest on the results of measurements with more intrinsic directional information.

Linear dichroism measurements can provide this type of directional information, and this technique has been used to determine the rotation of the chromophore transition dipole moment in the photointermediates from Batho to Lumi. The results showed that the transition dipole moment of the chromophore rotates through an angle of  $\sim 20^\circ$  when BSI is formed from Batho.<sup>16</sup> This comparatively large rotation is consistent with there being substantial motion of the C13 end of the polyene chain during BSI formation as suggested in the model described above. Note that such a large change in transition dipole direction requires a relatively large displacement of at least one end of the polyene chain, as is produced here by initial rotation about the C6-C7 bond followed by motion of the C13 end of the polyene. Equivalent motion at the C13 end, pivoted, for example, about C8-C9 or C10-C11 single bonds, has progressively less effect on the transition dipole moment direction. In effect, the larger the portion of the polyene chain that does not move, the more exaggerated the motion of the moving part must be to produce the observed overall change in the transition dipole moment orientation. Manipulation of simple structural models, such as those constructed here with Hyperchem, illustrates the difficulty of producing sufficient transition dipole rotation except with a model involving rotation at the C6-C7 single bond. Motion of the C13 end of the polyene when BSI is formed also agrees with FTIR results<sup>9a</sup> that show that the C=N stretching frequency changes in BSI relative to the value in the pigment and in Batho, indicating a change in Schiff base environment.

Finally, it should be noted that recent calculations of <sup>13</sup>C NMR chemical shifts<sup>17</sup> have placed the counterion on what corresponds to the left hand side of the polyene as viewed in Figure 5. Motion of the chromophore to the left would thus

reduce the counterion-chromophore distance in BSI, possibly accounting for its typically blue-shifted spectrum. That this leftward motion is interfered with by bulk at the C13 position may explain the absence of a blue shift (relative to the pigment) for the BSI of 13-ethylisorhodopsin (see Table 3). Given this steric interference with the normal BSI chromophore position, the observation of much slower BSI decay for this pigment seems reasonable. One simple model that can account for the observations here is that leftward motion of the polyene chain in BSI relieves some constraint on the right hand side of the chromophore (as pictured in Figure 5), which normally prevents protein motion. Alkyl substituents, especially 13-ethyl, interfere with completion of this motion, leading to residual interference with the motion on the right hand side of the chromophore. Detailed understanding of the structures involved, however, can only come from kinetic work with suitably engineered rhodopsin mutants.

Only one of the pigments studied here (locked 9-*trans*-rhodopsin) has been characterized on this time scale previously. In the previous study,<sup>10</sup> similar time dependent changes were observed, but the data were of insufficient quality to resolve two exponential processes. Further, at the time those measurements were conducted, the decay of Batho was assumed to be a simple one, direct to Lumi. Since that time, substantial progress has been made both in apparatus and in the understanding of the transduction mechanism prevailing on this time scale. While it can be argued that the extra 19,11-ethano ring structure provides constraints that preclude interpretation of results from this pigment in the same terms as the two ethyl pigments, the results show that strong similarities exist in the behavior of all three pigments on the time scale studied here. This shows that the ring constraint does not interfere intrinsically with the motion required for Batho decay independent of the effects of its added bulk. It also demonstrates that BSI formation does not require a significant twist around the 10-11 bond.

## Conclusions

The results indicate that free volume in the pocket near the 9-methyl comes into play during the decay of Batho to BSI. Later, the free volume near the C13 position stabilizes BSI. The picture that emerges is of a sequential process initiated at the C9 position and continued at the C13 end of the chain. If sufficient bulk is present, complete formation of BSI is interfered with, slowing the rate of the subsequent protein change leading to Lumi. Detailed understanding of the nature of the protein change that occurs depends on having a better structural model of the protein in this area. Such information should be obtainable from site-directed mutagenesis studies. Up to now, synthetic pigment studies have provided the best spatial picture of the pocket. Combination of those studies with kinetic measurements may add the additional dimension needed to unravel the mechanism of action of this important region of heptahelical receptors.

**Acknowledgment.** This work was supported by a grant from the National Institutes of Health (EY00983 to D.S.K.) and from the Fund for Basic Research (administered by the Israel Academy of Sciences and Humanities, to M.S.).

JA942330N

(15) Liu, R. S. H.; Asato, A. E.; Denny, M.; Mead, D. *J. Am. Chem. Soc.* **1984**, *106*, 8298-8300.

(16) Lewis, J. W.; Einterz, C. M.; Hug, S. J.; Kliger, D. S. *Biophys. J.* **1989**, *56*, 1101-1111.

(17) Han, M.; DeDecker, B. S.; Smith, S. O. *Biophys. J.* **1993**, *65*, 899-906.